Spatiotemporal Properties of Layer V Neurons of the Rat Primary Somatosensory Cortex

Asif A. Ghazanfar[1] and Miguel A.L. Nicolelis

Department of Neurobiology, Duke University Medical Center, Durham, NC 27710, USA
[1]Current address: Primate Cognitive Neuroscience Laboratory, Department of Psychology, 33 Kirkland Street, Rm 982, Harvard University, Cambridge, MA 02138, USA

Animals in their natural environments actively process spatiotemporally complex sensory signals in order to guide adaptive behavior. It therefore seems likely that the properties of both single neurons and neural ensembles should reflect the dynamic nature of such interactions. During exploratory behaviors, rats move their whiskers to actively discriminate between different tactile features. We investigated whether this dynamic sensory processing was reflected in the spatial and temporal properties of neurons in layer V of the 'whisker area' in the rat primary somatosensory cortex. We found that the majority of layer V neurons had large (8.5 ± 4.9 whiskers) spatiotemporal receptive fields (i.e. individual cells responded best to different whiskers as a function of post-stimulus time), and that the excitatory responses of surround whiskers formed a spatial gradient of excitation that seemed to reflect the greater use of the ventral and caudal whiskers during natural behaviors. Analyses of ensembles of layer V neurons revealed that single-whisker stimuli activated a portion of layer V that extends well beyond a single cortical column (average of 5.6 barrel cortical columns). Based on these results, we conclude that the rat primary somatosensory cortex does not appear to operate as a static decoder of tactile information. On the contrary, our data suggest that tactile processing in rats is likely to involve the on-going interactions between populations of broadly tuned neurons in the thalamocortical pathway.

Introduction

Ethologically relevant sensory signals typically have complex spatial and temporal structures, and animals can readily perceive and discriminate among these signals to guide their adaptive behavior. This suggests that the nervous system must be capable of processing complex, time-dependent signals very efficiently. For example, the timing and order of fundamental components of speech (syllables, phonemes, etc.) play a critical role in specifying the meaning of different words (Merzenich *et al.*, 1996). Neural circuits of the human temporal lobe are specialized to some degree to process these auditory signals rapidly (Damasio *et al.*, 1996). It is likely that in other sensory systems, the properties of neural circuits reflect their roles in decoding the spatiotemporal structure of signals in order to allow the subject to perceive and respond adaptively to them.

The active movement of sensory organs by animals during exploratory behaviors also incorporates time variation as an important component of sensory processing. For example, during active exploration of their environments, rats employ stereotypical movements of their facial whiskers to perceive differences in textures and shape (Carvell and Simons, 1990). It has been proposed that the time-dependent nature of neuronal receptive fields in the rat somatosensory thalamus reflects this active sensory processing (Nicolelis and Chapin, 1994). When rats are prevented from using their whiskers actively, their ability to discriminate textural features is diminished (Carvell and Simons, 1996), and the receptive field properties of thalamic neurons change considerably as well (Nicolelis *et al.*, 1996). Furthermore, lesions in the primary somatosensory (SI) cortex impair active tactile discrimination by rats (Hutson and Masterton, 1986). It remains unclear, however, how the physiological properties of cortical neurons reflect the dynamic nature of the sensory signals they are supposed to process.

The SI cortex of rodents is characterized by the clustering of layer IV neurons into aggregates known as 'barrels' (Woolsey and Van der Loos, 1970; Killackey, 1973). In the posteromedial portion of rodent SI cortex, the arrangement of barrels corresponds to the discrete matrix of whiskers on the snout of the animal. Each single barrel represents a structural unit that corresponds to a single, isomorphic whisker. Mapping studies have demonstrated that neurons within a cortical column, both above and below a barrel, respond preferentially to deflections of one 'principal' whisker (PW) and respond more weakly to adjacent whiskers surround whiskers (SWs) (Simons, 1978; Ito, 1981; Armstrong-James and Fox, 1987). Thus, each barrel cortical module seems to form the center of a cortical column that extends from layer I to the white matter (Durham and Woolsey, 1985; McCasland and Woolsey, 1988; Chmielowska *et al.*, 1989). As such, the rodent somatosensory pathway provides an excellent model system to study the spatial and temporal properties of cortical neurons following the activation of a discrete peripheral unit, the single whisker.

In the rodent SI cortex, little is known about the dynamic properties of single units or neural ensembles in cortical layers beyond the 'barrels', the clusters of neurons found in layer IV (Woolsey and Van der Loos, 1970; Killackey, 1973). Of particular interest are the infragranular layers, especially layer V. Layer V neurons receive inputs from all cortical layers, via their extensive basilar and apical dendrites, and are the major output layer, both intracortically and subcortically (Killackey *et al.*, 1989; Koralek *et al.*, 1990). Patterns of axonal projections and dendritic arbors of infragranular neurons are very different from those of supragranular or granular neurons (Ito, 1992; Hoeflinger *et al.*, 1995; Gottlieb and Keller, 1997). Thus, it is of significant interest to quantitatively examine the spatial and temporal properties of neurons in this layer of SI cortex. Such experiments would compliment the plethora of studies concerning the intrinsic properties of layer V neurons in slices of rodent SI cortex (Agmon and Connors, 1992; Gil and Amitai, 1996; Markram, 1997) [reviewed by Connors and Amitai (Connors and Amitai, 1995)]. In this paper, we examined the spatiotemporal properties of single neurons and neural ensembles in layer V of rat SI cortex under Nembutal anesthesia in response to single-whisker deflections using chronically implanted microwire arrays.

Materials and Methods

Animals and Surgical Procedures

Seven adult female Long–Evans rats (250–300 g) were used in these experiments. Details of surgical procedures have been described elsewhere (Nicolelis *et al.*, 1997). Briefly, animals were anesthetized with i.p.

injections of sodium pentobarbital (Nembutal, 50 mg/kg) and transferred to a stereotaxic apparatus. When necessary, small supplementary injections of sodium pentobarbital (~0.1 cm^3) were administered to maintain anesthesia during the surgery. Following retraction of the skin and soft tissue, a small, rectangular craniotomy was made over the primary somatosensory 'barrel' cortex using stereotaxic coordinates. Stainless-steel microwire arrays (NB Labs, Dennison, TX) were slowly lowered into the deep layers of SI cortex (~1200 μm in depth) and cemented to the animal's skull with dental acrylic. Each microwire array consisted of two rows of eight stainless-steel, Teflon-coated, 50 μm diameter microwires. The distance between the two rows of microwires was 1 mm and the distance between microwires within a row was 200 μm. Microwire arrays were always placed with the two rows oriented rostral–caudally within the rostral and medial portion of the posteromedial barrel field (to target the region isomorphic to the ventral and caudal whiskers). This approach allowed us to sample from an ~2 mm^2 region of SI cortex in each subject. The location of all microwires was assessed by qualitative receptive field mapping during surgical implantation and later confirmed by the quantitative response profiles of neurons and by localization in Nissl-stained sections.

Data Acquisition

Spike Sorting

Following a recovery period of 5–7 days, animals were anesthetized with sodium pentobarbital (50 mg/kg) and transferred to a recording chamber where all experiments were carried out. A head stage plug was used to connect the chronically implanted microwires to a preamplifier whose outputs were sent to a Multi-Neuronal Acquisition Processor (MNAP, Plexon Inc., Dallas, TX) for on-line multichannel spike sorting and acquisition (sampling rate = 40 kHz/channel). A maximum of four extracellular single units per microwire could be discriminated in real time using time–voltage windows and a principal component-based spike-sorting algorithm (Abeles and Goldstein, 1977; Nicolelis and Chapin, 1994). Previous studies have revealed that under our experimental conditions, ~80% of the microwires yield stable single units and an average of 2.3 single cortical units can be well-discriminated per microwire (Nicolelis *et al.*, 1997). Examples of waveforms and further details regarding acquisition hardware and spike sorting can be found elsewhere (Nicolelis and Chapin, 1994; Nicolelis *et al.*, 1997).

Recording Session and Whisker Stimulation

After spike sorting, the simultaneous extracellular activity of all well-isolated single units was recorded throughout the duration of all stimulation experiments. A computer-controlled vibromechanical probe was used to deliver innocuous mechanical stimulation to single whiskers on the mystacial pad contralateral to the microwire array implant. The independent stimulation of 24 whiskers was carried out per recording session per animal. Three hundred and sixty trials were obtained per stimulated whisker. Whiskers were stimulated in random order by positioning the probe just beneath an individual whisker, ~5–10 mm away from the skin. Extreme care was taken to ensure that only a single whisker was being stimulated at all times. A step-pulse (100 ms in duration) delivered at 1 Hz by a Grass 8800 stimulator was used to drive the vibromechanical probe. The output of the stimulator was calibrated to produce a ~0.5 mm deflection of whiskers. These deflections were made in an upward direction because it was easier to isolate single whiskers with our probe from a ventral approach. As previous studies have demonstrated that most SI cortical neurons have little or no directional selectivity (Ito, 1983; Simons and Carvell, 1989), we did not investigate the directional selectivity of layer V neurons. Stable levels of anesthesia were maintained by small supplemental injections of pentobarbital (~0.05 cm^3) and monitored through regular inspection of brain activity, breathing rates and tail-pinch responses.

Data Analysis

Firing Rate and Minimal Latencies

The minimal spike latency and the average evoked firing rate were estimated for each neuron using post-stimulus time histograms (PSTHs) and cumulative frequency histograms (CFHs). CFHs were used to measure the statistical significance and latency of sensory responses. These histograms depict the cumulative post-stimulus deviations from pre-stimulus average firing seen in the PSTHs. In other words, the CFHs describe the probability that the cumulative frequency distribution in the histogram differs from a random distribution, as computed by a one-way Kolmogorov–Smirnov test. Neuronal responses were considered statistically significant if the corresponding CFH indicated a $P < 0.01$. In CFHs of statistically significant responses, the minimal latencies were recorded as the time where an inflection point in these plots were seen; inflection points demarcated the initial change in firing rate (Nicolelis *et al.*, 1993a; Faggin *et al.*, 1997). These analyses were carried out on commercially available software (Stranger, Biographics, Inc.).

To facilitate the analysis of a large number of PSTHs, we later adopted a semi-automated method of measuring firing rate and latency, based on kernel density estimation (KDE). This approach has been used successfully by others to measure firing rates and latencies in neural data (MacPherson and Aldridge, 1979; Richmond *et al.*, 1987). This method is less sensitive to slight changes in the time of occurrence of individual action potentials from trial to trial and avoids bin-edge artifacts of conventional PSTHs (Richmond *et al.*, 1987). Software (written by Dr Mark Laubach, laubach@neuro.duke.edu) using KDE functions was developed in Matlab (Mathworks, Natick, MA). A graphical user interface allowed the user to inspect graphically and confirm or reject the results of the semi-automated analysis procedures using CFHs. In the KDE analysis, PSTHs were constructed using 1 ms bins for the epoch from 100 ms before to 100 ms after stimulus onset. Spike densities over this epoch were assessed using KDE. Neurons were included in subsequent analyses if the mean spike density after the stimulus was greater than the mean spike density before the stimulus. The kernel function for all analyses was the normal (Gaussian) probability density function. The smoothing parameter (the window- or band-width, h) was estimated adaptively. The general procedure for KDE was as follows: (i) an initial estimate of h was made as the minimum of the standard deviation and interquartile range for the distribution of spike times; (ii) kernel functions based on this estimate of h were placed at the observed data points; (iii) h was varied over the data points such that larger values for h were used in regions of relatively high spike density (i.e. the kernel is 'adaptive' to changes in firing rate); and (iv) the density estimates for the individual data points were integrated over the entire epoch to give an estimate of spike density over time.

The average minimal spike latency was assessed as follows: (i) the time of the first spike after the stimulus (i.e. the minimal spike latency) was found for each trial; (ii) spike densities were estimated for the 100 ms epoch prior to the stimulus and for the distribution of minimal spike latencies; (iii) the maximum spike density prior to the stimulus was subtracted from each point in the density estimate of minimal latency to correct for the neuron's rate of spontaneous discharge; (iv) the maximum value in the density estimate for minimal spike latency was taken as an estimate of minimal spike latency; and (v) time points at which the normalized cumulative distribution of the minimal spike latency was greater than 0.10 and 0.99 were taken, respectively, as estimates of the onset and offset of the neurons' instantaneous responses to the stimuli. These values (the onset and offset) account for the range of variability in minimal spike latencies over the collection of trials. The statistical significance of each neuron's response, in the form of PSTHs and cumulative frequency histograms (CFHs), was assessed for all whiskers stimulated.

Nearly identical results were obtained using both the commercially available software and the software we developed based on the KDE method for measurements of firing rate and latency. All results reported in this paper are based on the semi-automated KDE method.

Receptive Field Analysis

The rat whisker pad is conventionally divided into a matrix that is very similar across individual animals. Dorsal to ventral rows (A–E) and caudal to rostral columns (1–6) provide each whisker with a unique label (e.g. C3, E1), with straddler whiskers, located caudally between rows, labeled (from dorsal to ventral) α, β, γ and δ (for convenience, we rename these straddler whiskers A0, B0, C0 and D0 respectively). The whisker eliciting

the largest response from a neuron with the shortest latency is called the principal whisker (PW) and is used to define the center of the receptive field (CRF). Other whiskers that can elicit a significant response are called the surround whiskers (SWs), and together they constitute the surround receptive field (SRF). The receptive field size of a neuron was assessed by counting the number of whiskers that could elicit a statistically significant response. Because of the strict anatomical topography and vertical organization of SI cortex (Simons, 1978; Chapin, 1986; McCasland and Woolsey, 1988; Armstrong-James *et al.*, 1992), the CRF of a neuron provides a fairly accurate estimate of the location of an electrode within SI cortex. For example, if whisker E1 elicited the largest response from a neuron, then that neuron was in all likelihood recorded from a microwire located in the E1 cortical column defined by the E1 barrel or surrounding septum. We used this information to determine the portion of SI cortex and the number of barrel 'columns' sampled by our microwire arrays in each animal during our recordings which were confirmed later by histology (Fig. 1). This information also provided an anatomical reference from which to base our cortical activation analyses upon (see below).

Spatiotemporal Receptive Fields

As described in the Results, many SI cortical neurons exhibited time-dependent shifts of their RF centers along the caudal to rostral and/or dorsal to ventral dimensions. For this analysis, a single neuron's response to each whisker was divided into the following epochs: 8–12, 12–16, 16–20, 20–24, 24–28, 28–32, 32–36 and 36–40 ms post-stimulus. In each epoch, the whisker that elicited the greatest response (measured by spike counts) was defined as the 'center'. Because the 'center' whisker often varied as a function of post-stimulus time, we were able to map the 'spatiotemporal' CRF for most neurons. This approach is nearly identical to the 'response plane' techniques used to map spatiotemporal RFs in the visual system (Stevens and Gerstein, 1976; Dinse *et al.*, 1991), except that here only one random stimulus sequence from the ~5 × 5 matrix of whisker locations is given for each neuron because the trials cannot be interleaved due to technical limitations. In other words, one whisker is stimulated for 360 trials, and then the vibromechanical probe is moved to another whisker for 360 trials.

To determine the directional bias of each spatiotemporal RF, we measured the maximum distance over which the new 'CRF' moved from the shortest latency RF center in number of whiskers. While a spatiotemporal RF may travel in multiple directions, it is the direction that is the farthest away from the short latency PW that we labeled as the 'directional vector' of the spatiotemporal RF. Five categories of spatiotemporal RFs were defined based on their direction of shift: dorsal-to-ventral (DV), ventral-to-dorsal (VD), rostral-to-caudal (RC), caudal-to-rostral (CR) and unclassifiable (UC, those that have no clear directional vector). A subclass of spatiotemporal RFs were categorized as 'reverberatory' because the CRF whisker returned through a previously traversed center. The 'complexity' of a spatiotemporal RF was measured by counting the number of new centers a neuron traveled through over 40 ms of post-stimulus time. The maximum complexity that could be measured was eight (the number of time epochs used in this analysis).

Cortical Activation

We were able to measure the average amount of SI cortex recruited over time in response to single-whisker deflections. Color-coded three-dimensional matrices represented the post-stimulus firing of SI ensembles according to their location on the 2 × 8 microwire arrays. The data were plotted on consecutive 4 ms post-stimulus time epochs (8–12, 12–16, 16–20, 20–24, 24–28, 28–32, 32–36 and 36–40 ms) (see Fig. 10). By using the information about PW gathered from the receptive field analysis, we were able to translate the position of each microwire according to its barrel cortical column location. This allowed us to measure the distribution of cortical activation within the infragranular layers referenced to the overlying barrel field and pool our results across animals. In cases where more than one neuron were recorded from an electrode, we did not treat each neuron separately. For our analyses, the barrel cortical column was considered active no matter which neuron from that microwire was responsible for that activation. The amount of SI cortical activation following single-whisker stimulation was quantified by counting the number of barrel columns that were active in each time

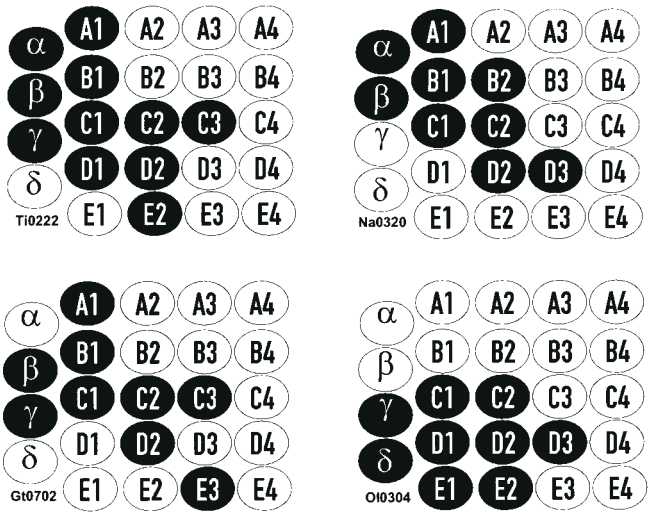

Figure 1. Four representative examples of the cortical sampling obtained from our chronic microwire arrays. Arrays of 16 microwires were implanted in the whisker region of the rat primary somatosensory cortex. Regions shaded in black indicate that at least one microwire was located in that barrel cortical column. All microwires were in layer V, as confirmed by response profiles and by histological analysis of Nissl-stained sections.

epoch. For the purposes of this analysis, we defined significant activity as being at least 4 SDs above pre-stimulus baseline activity. Parametrically varying this criterion from 2 to 8 SDs only minimally affected the magnitude of the response (A.A. Ghazanfar and M.A.L. Nicolelis, unpublished observations).

Dependent and independent *t*-tests and chi-square measurements were used to measure the significance of comparisons across conditions. A $P < 0.05$ was considered significant.

Histology

The laminar depth of each microwire was confirmed for every animal through examination of Nissl-stained sections. After completion of recording sessions, animals were given a lethal dose of pentobarbital and then perfused intracardially with 0.9% saline solution followed by 4% formalin in 0.9% saline. Brains were post-fixed for a minimum of 24 h in the same fixative solution. Coronal sections of the whole brain (80 μm) were cut on a freezing microtome. Sections were then counterstained with cresyl violet to reveal the modular structure of barrel cortex (Killackey, 1973). Microwire tracks and tip positions were located using a light microscope. Because microwires were chronically implanted and remained in the brain for several days, electrode tracks and tip positions could be readily identified by linear tracks of Nissl-positive glial nuclei, obviating the need for electrical lesions.

Results

Seven rats provided a total sample of 197 layer V SI cortical neurons. We were able to perform parallel recordings of small ensembles of well-isolated single neurons, distributed across a ~2 mm^2 extent of the SI cortex. Our off-line analysis revealed that neural ensemble sizes were, on average 28.1 neurons, and ranged from 16 to 45 single neurons (Nicolelis *et al.*, 1997). From each 16 microwire array, we were able to sample neurons from an average of 8.5 barrel columns. Figure 1 shows four representative examples of the sampling obtained by our microwire arrays. The location of each microwire is indicated by the regions shaded in black. The variability in the number of barrel cortical columns sampled could be related to several variables including the size of the animal (and therefore the inaccuracy of stereotaxic coordinates), the twofold variation in barrel field size

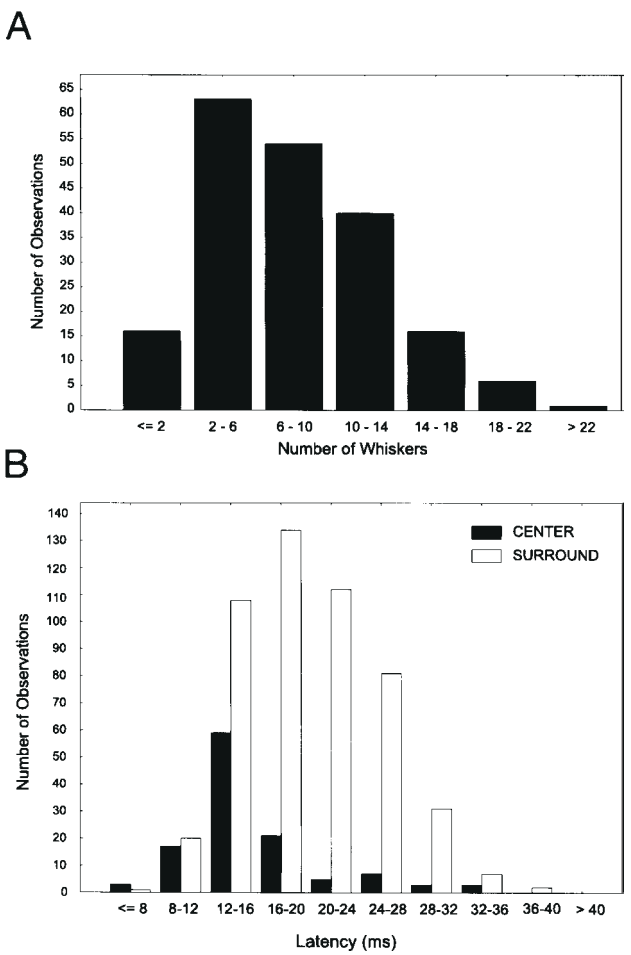

Figure 2. (*A*) Distribution of receptive field sizes for 118 layer V neurons from SI cortex. Receptive field sizes were measured by counting the number of whiskers that elicited statistically significant responses from a given neuron. The average receptive field size was 8.5 ± 4.9 (mean ± SD) and ranged from 1 to 24 whiskers. (*B*) Distribution of the minimal latencies neuronal responses for principal whisker stimulation ($n = 118$; black bars) and surround whisker stimulation ($n = 496$; gray bars). The average latency for principal whiskers was 16.0 ± 5.4 ms (mean ± SD; range 7.0–35.0ms). The average latency for surround whiskers was 20.2 ± 5.4 (mean ± SD; range 7.1–38.5 ms). The difference between principal and surround whisker latencies was highly significant ($P < 0.00001$).

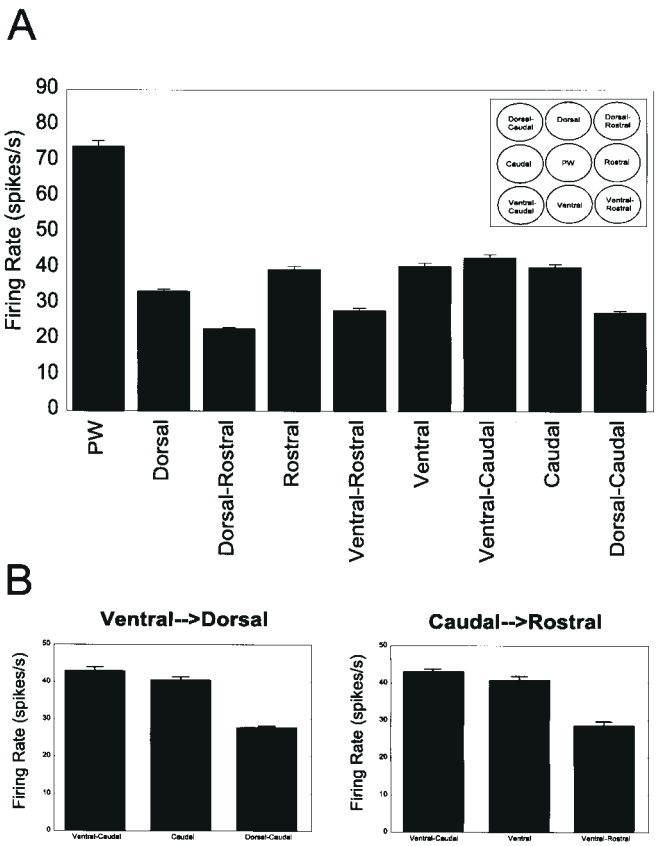

Figure 3. (*A*) Comparison of the firing rates between the principal whisker and the surround whiskers immediately adjacent to the principal whisker ($n = 118$ neurons). Dorsal to ventral and rostral to caudal distinctions are all relative to the principal whisker. (*B*) A spatial gradient of excitation exists in the ventral to dorsal direction (left panel) and caudal to rostral direction (right panel). (Left panel) The ventral–caudal and caudal surround whisker responses were significantly greater than the dorsal–caudal surround whisker's response ($P < 0.05$ and $P < 0.05$ respectively). (Right panel) The ventral surround whisker responses were significantly greater than the ventral–rostral surround whisker responses ($P < 0.05$). Inset shows relationship between surround whiskers and the principal whiskers. Error bars show 1 SEM.

across individual animals (Riddle and Purves, 1995) and the variability in individual barrel column sizes (Zheng and Purves, 1995). Nevertheless, microwire arrays consistently targeted several barrel cortical columns, in a continuous fashion, representing the large, caudal whiskers. Our experiments focused on these whiskers because they are the ones that appear to be most actively involved during tactile discrimination tasks (Carvell and Simons, 1990). Histological analysis of Nissl-stained sections confirmed that all recordings were obtained from neurons located in layer V.

The chronic microwire implants permitted us to record populations of well-isolated single neurons for several hours at a time (Nicolelis *et al.*, 1997), allowing the use of a large stimulus set (24 whiskers; whiskers A0–A4, B0–B4, C0–C4, D0–D4 and E1–E4) and a large number of trials (360) per site. Since many neurons were recorded in parallel, the impact of some sources of non-stationarity in recording could be greatly diminished.

Quantitative Measurement of Receptive Field Sizes and Minimal Latencies in Layer V

Quantitative and statistical analyses of neuronal responses were used to determine the significance of evoked responses of each neuron to the 24 different whiskers. As reported previously (Simons, 1978; Ito, 1981; Chapin, 1986; Armstrong-James and Fox, 1987), the vast majority of layer V neurons had multi-whisker RFs. Figure 2*a* shows the distribution of RF sizes obtained in this study (8.5 ± 4.9, mean ± SD whiskers). There was considerable heterogeneity among layer V RFs under pento-barbital anesthesia, as some neurons responded to only one or two whiskers, while others were able to respond to nearly the entire whisker pad (range = 1–23 whiskers).

By definition, the PW of each neuron elicited the strongest response at the shortest latency compared to other whiskers. The distributions of minimal latencies for PWs ($n = 118$) and SWs ($n = 496$) are shown in Figure 2*b*. The mean minimal latency for PW responses was 16.0 ± 5.4 ms (mean ± SD; range 7.0–35.0 ms), and the mean minimal latency for SWs was 20.2 ± 5.4 ms (mean ± SD; range 7.1–38.5 ms). The difference between PW and SW latencies was highly significant ($t(117) = -4.63$, $P < 0.00001$).

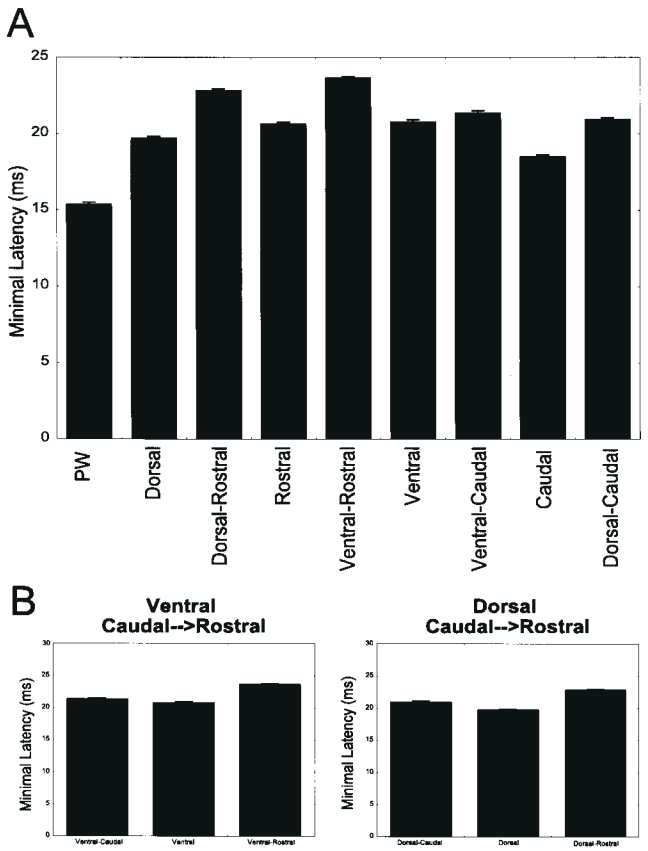

Figure 4. (*A*) Comparison of the minimal latencies between the principal whisker and the surround whiskers immediate adjacent to the principal whisker ($n = 118$). (*B*) Only a limited spatial gradient of latencies emerges. (Left panel) The rostral-most SWs had longer minimal latencies when compared to those whiskers caudal to them. The ventral–rostral SW latency was longer than the ventral SW (23.3 versus 20.8 ms, $P < 0.05$). (Right panel) Similarly, the dorsal–rostral SW latency was longer than the dorsal SW (23.1 versus 18.8 ms, $P < 0.01$). Error bars show 1 SEM.

Patterns of Excitation Around the Principal Whisker

The relationships between the response magnitudes and latencies of SWs and their location relative to the PW were investigated in order to reveal potential spatial biases as seen in the supragranular and granular layers (Simons and Carvell, 1989; McCasland *et al.*, 1991). Since rats naturally use their caudal and ventral whiskers, which tend to be the largest, to actively 'whisk' objects during natural behavior and tactile discrimination tasks (Carvell and Simons, 1990), we expected that they would demonstrate larger responses and shorter latencies as SWs than more rostral SWs. We tested this by comparing the response magnitudes and minimal latencies of the SWs immediately adjacent to the PW. Figures 3 and 4 compare the mean and standard error of firing rates and minimal latencies for principal and adjacent surround whiskers. This analysis was based on the responses of 118 neurons from five animals pooled together. Because the SRFs of layer V SI cortical neurons are not always symmetrically distributed around the PW (Simons, 1978; Chapin, 1986), the number of observations for each pairwise comparison of SWs was variable.

A comparison of the firing rates of SWs revealed a consistent pattern of excitation around the PW (Fig. 3*A*,*B*). The ventral–caudal SW's response was significantly greater than the following dorsal SWs: dorsal–caudal to the PW [$t(22) = 2.23$, $P < 0.05$] and the SW dorsal to the PW [$t(29) = 2.09$, $P < 0.05$]. The ventral SW response magnitude was significantly greater than the dorsal–caudal SW [$t(24) = 2.60$, $P < 0.05$], the ventral–rostral SW [$t(37) = 2.20$, $P < 0.05$], and the dorsal–rostral SW [$t(19) = 2.94$, $P < 0.01$]. The caudal SW elicited a significantly greater response than the dorsal [$t(30) = 2.37$, $P < 0.05$], dorsal–caudal [$t(26) = 2.35$, $P < 0.05$], and ventral–rostral [$t(37) = 2.20$, $P < 0.05$] surround whiskers. Figure 3*B* examines these relationships more closely by comparing the responses of the ventral–caudal SW relative with those SWs dorsal to it (left panel) and to those SWs rostral to it (right panel). The ventral–caudal SWs had consistently larger response magnitudes. In keeping with this emerging pattern, the dorsal SW and the rostral SW responses were both greater than the dorsal–rostral response [$t(20) = 3.25$, $P < 0.005$ for dorsal SW; $t(20) = 2.35$, $P < 0.05$ for rostral SW]. Thus, we found that the ventral and caudal SWs had larger response magnitudes than the dorsal and rostral SW. This gradient is consistent with the activity gradients seen in 2DG studies of barrel cortex (McCasland *et al.*, 1991) and the inhibitory spatial gradients observed following sequential, multiwhisker integration in the granular layers (Simons and Carvell, 1989; Brumberg *et al.*, 1996).

A similar comparison of the minimal latencies for the SWs did not reveal a similar spatial gradient of temporal activation (Fig. 4*A*,*B*). Instead, only a limited pattern emerges such that the rostral-most SWs had longer minimal latencies when compared to those whiskers caudal to them (Fig. 4*B*). The ventral–rostral SW latency was longer than the ventral SW [23.3 versus 20.8 ms, $t(37) = 2.65$, $P < 0.05$]. Similarly, the dorsal–rostral SW latency was longer than the dorsal SW [23.1 versus 18.8 ms, $t(20) = 2.85$, $P < 0.01$]. Thus, while there is a clear spatial gradient for response magnitudes, there appears to be only a rough gradient, from caudal to rostral, for minimal latencies.

Spatiotemporal RF Properties of Cortical Neurons

As described above, layer V SI cortical neurons had multiwhisker RFs, with a wide range of response magnitudes and latencies for the SWs. The distribution of response latencies to center and surround whiskers was clearly bimodal (Fig. 2*B*); thus, an SI cortical neuron with a multiwhisker RF would respond to the PW and SWs at different times, defining a 'spatiotemporal RF', as has been found for VPM neurons in the rat (Nicolelis and Chapin, 1994). While stimulation of the PW always elicited the shortest latency response, the response latencies for SWs were not as predictable. We characterized these time-dependent RF dynamics for all cortical neurons, and demonstrated that for a majority of these neurons, the spatial structure of their RFs changed as a function of time.

The time-dependent nature of these RF dynamics can best be visualized using three-dimensional graphs. Figure 5 depicts the 'raw' spatiotemporal RFs of two different neurons from different animals. For the neuron in Figure 5*A*, the RF shifted from its PW (whisker C2 in the first 8–12 ms) to a more caudal part of the whisker pad (whisker C1, 12–16 ms), and finally to a rostral and ventral location over whisker E3. The neuron in Figure 5*B* also had whisker C2 as its PW at 8–12 ms, but then it moved caudally to C1 at 12–16 ms. From there, the neuron's RF traveled ventral to D1 and then finally to whisker E3. For both of these neurons, there was no significant sensory evoked activity beyond 28 ms post-stimulus time. In a subset of these experiments, we remapped the spatiotemporal RFs of neurons several hours later and found that their structure was extremely stable (data not shown); in other words, their spatial and temporal complexity

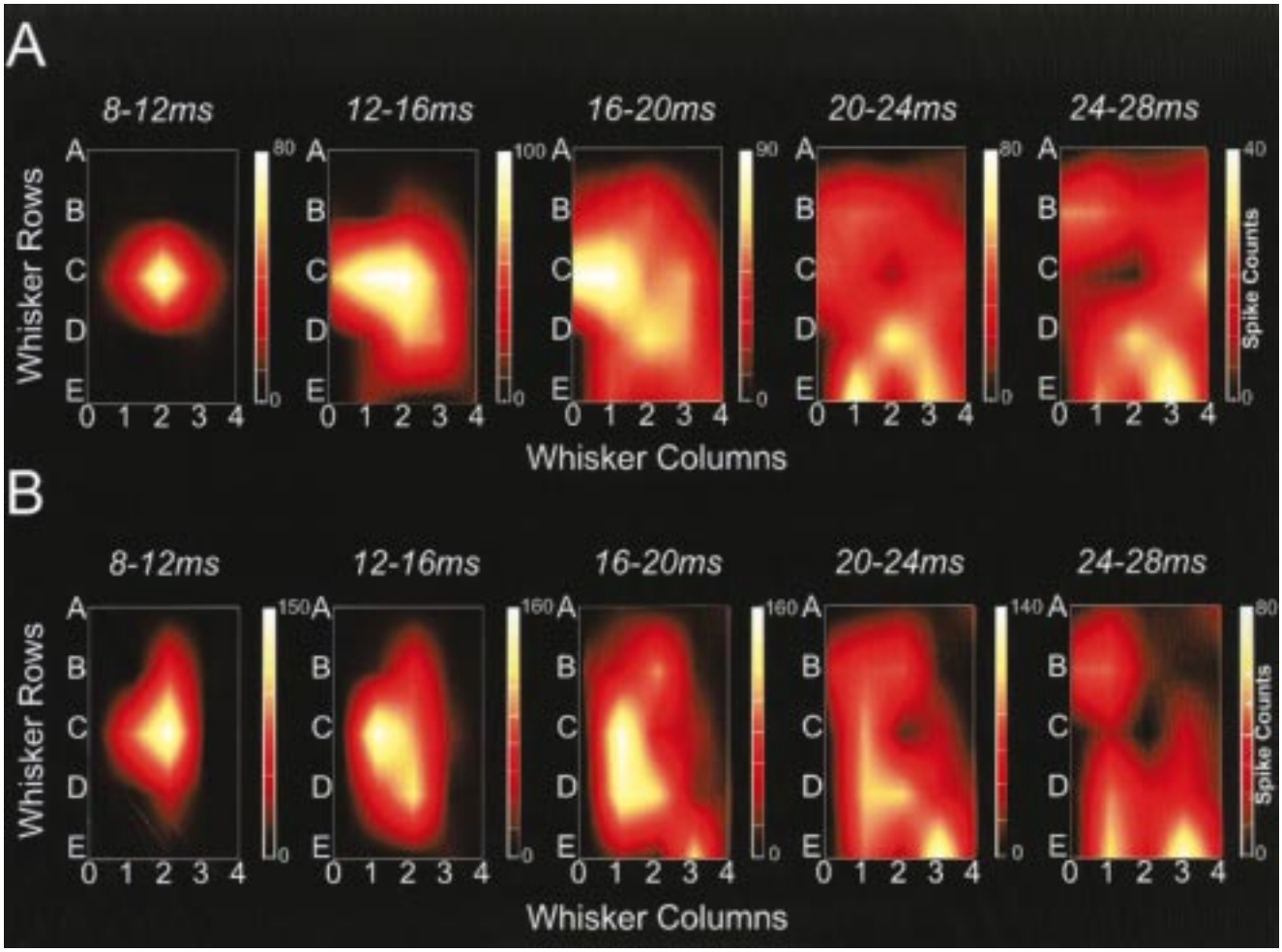

Figure 5. Two cortical spatiotemporal receptive fields from two different animals. Here, each color panel represents the matrix of whiskers on the mystacial pad of the animal (whisker columns – or 'arcs' – are on the *x*-axis, and whisker rows on the *y*-axis) for a given 4 ms epoch of post-stimulus time. The *z*-axis (color) represents the cell's stimulus-evoked spike count for each stimulated whisker. Notice that for each panel the *z*-axis is different. A fourth dimension, post-stimulus time, was represented by plotting a sequence of these three-dimensional graphs, each representing a 4 ms time epoch. Within a particular time epoch, the center is defined as the whisker eliciting the greatest response magnitude (measured in spike counts), but other SWs may continue to give significant responses. It can be seen that the RF centers of both of these neurons shift as function of time. See Results for a full description of these receptive fields.

was not the result of trial-to-trial variability. These results indicate that a neuron's RF can shift as a function of post-stimulus time.

Direction of RF Shifts

The patterns of these SI cortical spatiotemporal RFs varied widely, unlike those reported for the VPM which shifted only in a caudal to rostral direction or not at all (Nicolelis and Chapin, 1994). We analyzed the directional biases of each spatiotemporal RF by measuring the maximum distance the 'new' RF centers traversed from the PW location (highest response magnitude, shortest latency response) as a function of post-stimulus time. Four categories of directions were defined: rostral-to-caudal (RC), caudal-to-rostral (CR), dorsal-to-ventral (DV) and ventral-to-dorsal (VD). Neurons whose RFs traversed an equal distance in two or more directions were defined as 'unclassifiable' (UC). Several more examples of spatiotemporal RFs and their directional biases can be seen in Figure 6. In this figure, each panel represents the matrix of whiskers on the whisker pad and the vector indicates the direction and magnitude of the RF shift. Out of the 197 neurons in our sample, 175 (88.8%) exhibited time-dependent shifts in their RF centers, while 22 (11.2%) did not. Of those with spatiotemporal RFs, 17.7% were RC shifters, 16.0% CR shifters, 23.4% DV shifters and 6.3% VD shifters. The remaining 36.6% (64/175 neurons) could not be classified as having a single or unequivocal directional bias. Figure 7*A* demonstrates that across seven animals, there were roughly equal numbers of RC-, CR- and DV-shifting neurons; however, the number of VD-shifts was significantly less than RC-shifts [$t(6) = -3.15$, $P < 0.05$] and DV-shifts [$t(6) = 3.23$, $P < 0.05$].

Another class of neurons exhibited 'reverberatory' spatiotemporal RFs, since their spatiotemporal RFs were characterized as having centers that traversed a particular whisker location more than once (i.e. they would turn back, or 'reverberate'). Examples of these are depicted in Figure 8. For example, in the first panel, the center RF starts in D2, moves ventrally to E2 and then goes back to D2 before travelling dorsally to C2. Reverberatory spatiotemporal RFs comprised 14.9% of the 175 neurons with dynamic RF properties.

Another measurement used in the analysis of the organization of spatiotemporal RFs was 'complexity'. Complexity ('c', in the

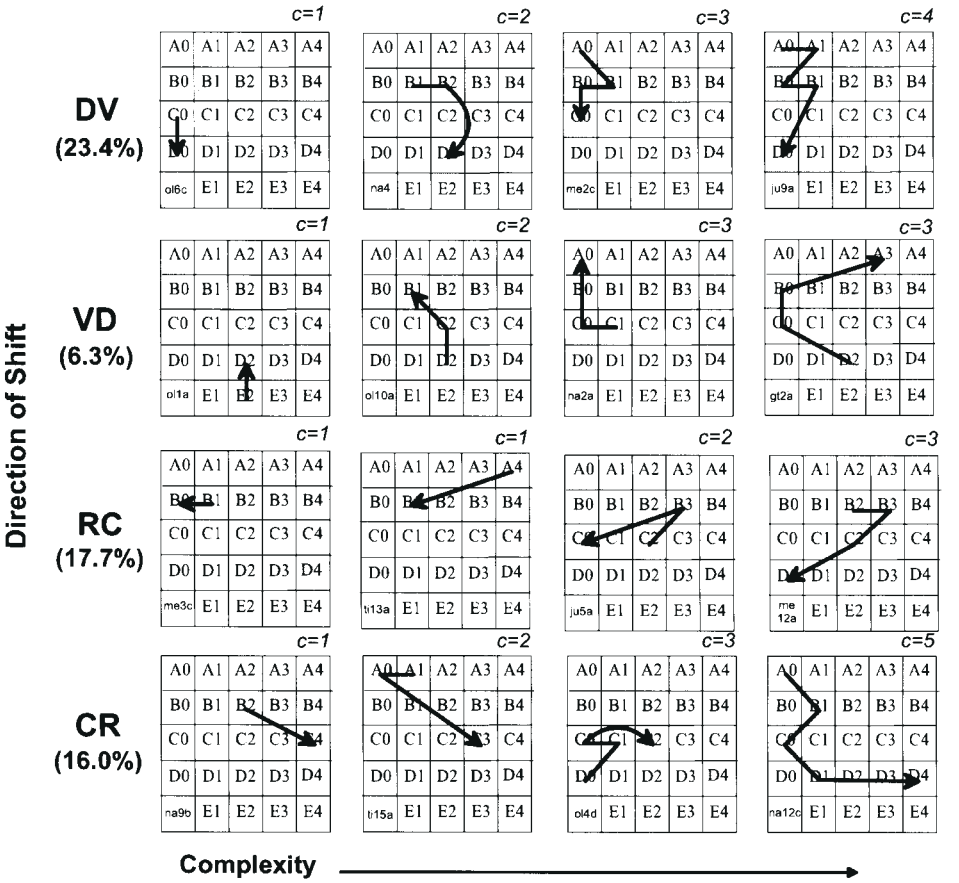

Figure 6. Sixteen examples of spatiotemporal receptive fields from six different animals classified according to directional bias and complexity. Each matrix represents the whisker pad, and the arrow represents only the direction of movement of the RF center over post-stimulus time; the shape of the trajectory represents the shape changes of the RF over post-stimulus time. The complexity (c) refers to the number of new RF centers a neuron went through over eight 4 ms post-stimulus time epochs. Directional biases were determined by measuring the direction in which the RF traveled maximally. Complexity was measured by counting the number of new centers an RF traversed. Percentages under each label indicate the frequency of each RF category in our sample. DV, dorsal-to-ventral; VD, ventral-to-dorsal; RC, rostral-to-caudal; CR, caudal-to-rostral; c, complexity.

upper right hand corner of each matrix in Figure 6) is defined as the number of new RF centers a neuron goes through *after* the PW. For example, a neuron that has a static CRF will have a complexity of zero, while a neuron whose CRF moves through two different whiskers over the eight time epochs would have a complexity of 2. The maximum complexity is 8 because that is the number epochs we used to analyze these data. Figure 7*B* shows the distribution of RF complexity seen in our data. For 197 neurons, the average complexity was 2.36 ± 1.52 (mean ± SD) and the range was 0–7.

Relationship Between the Principal Whisker and Spatiotemporal RFs

Was the directional class of spatiotemporal RF related to the location of the PW? The relationship between the location of the PW with the type of spatiotemporal RF that a particular neuron exhibited was examined by grouping the neurons according to which whisker column or row the PW belonged to. In Figure 9*A*, the normalized distribution for each type of spatiotemporal RF is categorized according to which whisker column the PW belongs to; in other words, the location of the PW was binned according to its caudal-to-rostral position on the whisker pad. A neuron whose PW was a straddler whisker (e.g. A0, B0, C0 or D0) would be placed in the 'column 0' bin, while a neuron whose PW was in the first (most caudal) column of whiskers would be placed in the 'column 1' bin, etc. Overall, neurons with PWs in column 0 or 1 had proportionally more spatiotemporal RFs that shifted in the DV direction, while PWs in columns 2 and 3 had proportionally more spatiotemporal RFs that shifted in the rostral-to-caudal direction. A chi-squared test for independence revealed that the distributions of spatiotemporal RF types between columns 0 and 1 versus columns 2 and 3 were significantly different (column 0 versus column2, $P < 0.0005$; versus column 3, $P < 0.005$; column 1 versus column 2, $P < 0.01$; versus column 3, $P < 0.05$).

In Figure 9*B*, the standardized distribution for each type of spatiotemporal RF is binned according the dorsal-to-ventral position of a neuron's PWs on the whisker pad (rows B–E). The more dorsal whisker rows, B and C, had proportionally more DV spatiotemporal RFs; row D had mostly RC spatiotemporal RFs; and the E row had mostly VD spatiotemporal RFs.

Overall, these analyses suggest that the direction of the spatiotemporal RFs is dependent upon the location of its PW (i.e. its shortest latency RF center). If a neuron's PW is located in column 0, column 1 or row B, then it is likely to have a DV spatiotemporal RF. If a neuron's PW is in column 2, column 3 or row D, then it is likely to have a RC spatiotemporal RF. In a limited manner, one can predict the type of spatiotemporal RF a neuron is likely to exhibit based upon edge-effects. For example, if a neuron's PW is whisker A0, then the directional bias of the spatiotemporal RF is limited, because of the edge-effects, to either DV or CR. Nevertheless, neurons whose PWs were in

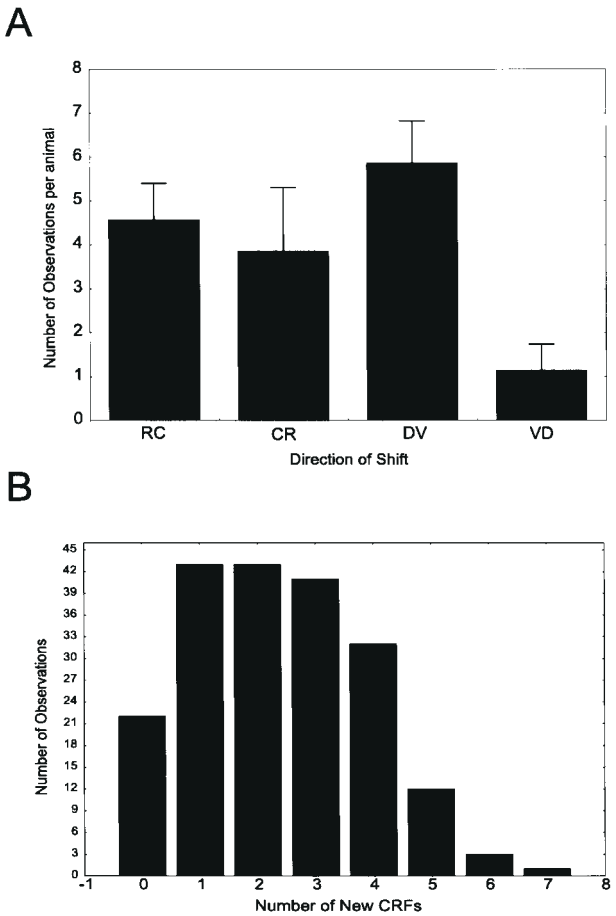

Figure 7. (*A*) Proportion of spatiotemporal receptive field types per animal. The *x*-axis represents the directional category of the RF; the *y*-axis represents the average number of observations seen per animal. Across seven animals, there were roughly equal numbers of RC-, CR- and DV-shifting neurons; however, the number of VD-shifts was significantly less frequent than RC-shifts [$t(6) = -3.15$, $P < 0.05$] and DV-shifts [$t(6) = 3.23$, $P < 0.05$]. DV, dorsal-to-ventral; VD, ventral-to-dorsal; RC, rostral-to-caudal; and CR, caudal-to-rostral. Error bars show 1 SEM. (*B*) Distribution of receptive field complexity. Complexity refers to the number of new centers an RF travels through over eight 4 ms epochs of post-stimulus time. The *x*-axis refers to the number of new possible center RFs (0 = no shift in RF center over time); the *y*-axis is the number of observations. For 197 neurons, the average complexity was 2.36 ± 1.52 (mean ± SD) and the range was 0–7.

column 0 were not distributed equally among the DV and CR categories; the majority were of the DV type.

In summary, we found that the large, asymmetrical RFs of layer V SI cortical neurons and the diverse minimal latencies for surround whiskers defined complex spatiotemporal RFs – RFs whose centers varied as function of post-stimulus time. Four classes of spatiotemporal RF types could be characterized based on directional biases of the RF movement, and these biases were dependent upon the location of the PW.

Cortical Activation Following Single-whisker Deflections

We characterized the large-scale spatiotemporal activity across a large portion of SI cortex following single-whisker deflections. Previous studies of cortical activation have focused on supragranular and/or granular layers of barrel cortex using imaging techniques (Kleinfeld and Delaney, 1996; Masino and Frostig, 1996; Peterson *et al.*, 1998) or have been inferred from serial reconstructions of microelectrode penetrations (Armstrong-James *et al.*, 1992). Here, we were able to take advantage of both the temporal resolution of single-unit recordings and the relatively large spatial resolution afforded by the use of chronic microwire arrays (~2 mm^2, see Materials and Methods) positioned in layer V.

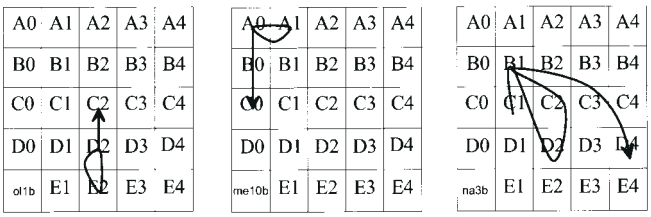

Figure 8. Reverberatory spatiotemporal receptive fields. Three spatiotemporal RFs are depicted here in the same format as in Figure 6. Note, however, that these RFs travel back through an RF center that was previously traversed, i.e. they reverberate. These neurons constitute 14.9% of the 175 neurons that had spatiotemporal RFs.

In order to reveal the spatial pattern and extent of cortical activity, we first quantitatively mapped the RF for each neuron sampled by each microwire in the array. By taking advantage of the known vertical organization of the rat barrel cortex (Simons, 1978; Chapin, 1986; Armstrong-James *et al.*, 1992), we then used the PW of each neuron to infer the anatomical location of the microwire relative to the overlying barrel field (Fig. 10, middle panel). For example, the neuron '1a' recorded from microwire 1 in Figure 10 had an RF whose PW was E3; we surmised that any activity on this microwire was in the E3 barrel cortical column (below the layer IV E3 barrel). Based on this approach, we took the significant activity (at least 4 SDs above baseline activity) across the microwire array for a given time epoch and translated it into activity across barrel cortical columns (Fig. 10, right panel). In some instances, as seen for some microwires in Figure 10 (middle panel), two or more neurons could be isolated from a single microwire and sometimes these neurons had different PWs; in these cases, we presumed that the microwire was located in an inter-barrel region below layer IV.

Figure 11 depicts two examples, from two different animals, of layer V SI cortical activation following stimulation of a single whisker. It can be seen that, in the first 8–12 ms post-stimulus, the activated barrel cortical columns were those isomorphic to the stimulated whisker as well as an adjacent barrel column. This activity then spread in many directions across the cortex to include many adjacent barrel columns, covering a distance of up to four barrel columns horizontally (Fig. 11*A*) or vertically (Fig. 11*B*). The peak of activation, in terms of number of barrel columns activated, occurred around 16–24 ms in both examples and then rapidly declined. In our analysis, it was important to make sure that each whisker had an equal number of barrel cortical columns it could activate; otherwise, our results would be skewed towards greater activation by some whiskers simply due to a sampling bias. Since we were unable to sample from the exact same set of barrel cortical columns across different animals (Fig. 1), we picked five animals that had the most overlap of sampling. A chi-square test of the distribution of microwire sites for these five animals determined that following barrel cortical columns were sampled evenly: B1, B2, B3, C1, C2, C3, D1, D2, D3, E1, E2 and E3 (no significant difference when compared to a flat distribution: $\chi^2 = 0.506$, $df = 11$, $P = 0.9999$). From this set of whiskers, we focused on a subset of these whiskers, C1–C3 and D1–D3 for subsequent analyses because their corresponding barrel columns were evenly sampled *and* the barrel columns

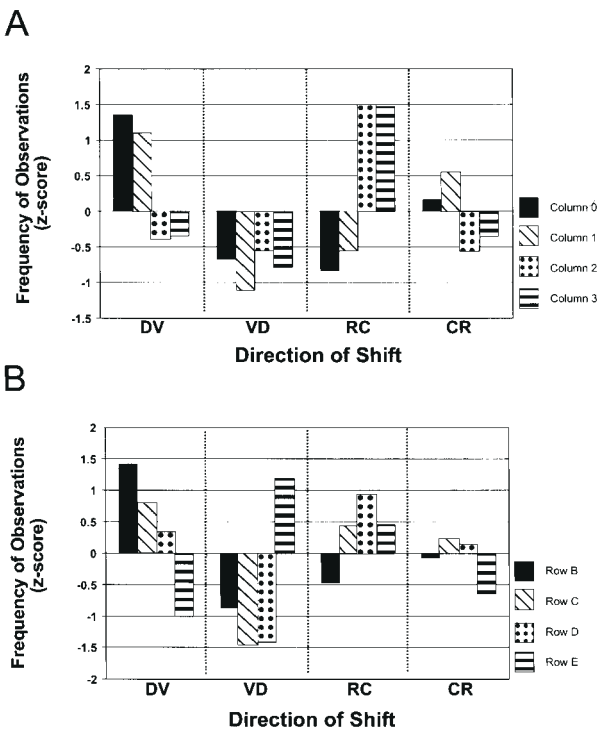

Figure 9. Relationship between spatiotemporal receptive fields and the location of principal whisker. Here, for each category of principal whisker location (either in columns or rows), the distribution of different spatiotemporal RF types was normalized and plotted. (*A*) The normalized distribution for each type of spatiotemporal RF is categorized according to which whisker column the PW belongs to. For example, a neuron whose PW was a straddle whisker (e.g. A0, B0, C0 or D0) would be placed in the 'column 0' bin, while a neuron whose PW was in the first (most caudal) column of whiskers would be placed in the 'column 1' bin, etc. Neurons whose principal whiskers were in the caudal part of the whisker pad tended to have spatial temporal RFs that shifted in the DV direction, while neurons whose principal whiskers were in the rostral part of the whisker pad shifted in the RC direction most often. (*B*) The normalized distribution for each type of spatiotemporal RF is categorized according to which whisker row the PW belongs to. Here, RFs whose principal whiskers were in the dorsal part of the whisker pad tended to shift in the DV direction, while RFs whose principal whiskers were in the ventral part of the whisker pad had RFs that shifted in the VD direction. DV, dorsal-to-ventral; VD, ventral-to-dorsal; RC, rostral-to-caudal; CR, caudal-to-rostral.

immediately adjacent to them, dorsally and ventrally, were also evenly sampled. These controls allowed us to circumvent a spatial bias in the analyses of cortical activation due to uneven sampling.

Next, the amount of SI cortex activated by different whiskers in terms of number of barrel cortical columns was measured. This was done by simply counting the maximum number of barrels activated in any given epoch of time. There were no significant differences in the peak number of barrel columns activated by the six different whiskers (Fig. 12*A*). On average, 5.6 barrel columns (~65% of the area sampled by our microwire arrays) were activated no matter which of the six whiskers was deflected. Figure 12*B* shows the temporal evolution of cortical activation following single-whisker deflections. The average number of barrel columns activated by a given whisker within a 4 ms post-stimulus time epoch was calculated and pooled together. Although significant cortical activity is present from 8 to 40 ms post-stimulus, the peak of this activation occurred during the 20–24 ms post-stimulus time epoch, where an average of 4.1 barrels were active. These results suggest that information available to SI cortex for location of a stimulus on the whisker pad is distributed over a large extent of SI cortex for several tens of milliseconds and peaks at ~20 ms.

Discussion

We analyzed the responses to simple single-whisker stimuli in both space and time from populations of well-isolated single layer V neurons from a 2 mm^2 region of the posteromedial barrel subfield of SI cortex in each animal. We found that 88.8% of layer V SI cortical neurons have large, asymmetrical RFs that are defined by a moving center and an excitatory gradient of surrounding responses. The center of these spatiotemporal RFs were found to shift in many different directions across the whisker pad. Neural ensemble recordings revealed that a large portion of SI cortex is activated when any single whisker is deflected. These recordings also revealed that the caudal whiskers activate more of SI cortex and at a shorter latency than rostral whiskers. Finally, to some degree the spatiotemporal neural ensemble response could be used to discriminate the location of single whisker stimulus.

Technical Considerations

Layer V of the rat somatosensory cortex contains many different morphological and physiological types of neurons (Amitai and Connors, 1995; Schwindt *et al.*, 1997), including differences between neurons in sublayer Va and Vb (Wise and Jones, 1977). Physiologically, it has been shown that layer Va neurons do not have a clear center–surround organization because there are no significant differences between the magnitude of their responses to the PW versus SWs (Armstrong-James *et al.*, 1992). A potential complication in the interpretation of that study is that urethane-anesthetized rats were used (Armstrong-James *et al.*, 1992), and it has been shown that urethane anesthesia increases the magnitude of responses to both PWs and SWs (Simons *et al.*, 1992). For layer Vb neurons, on the other hand, responses to the PW can be clearly distinguished from SW responses (Ito, 1985; Armstrong-James *et al.*, 1992). In our analysis of the spatial and temporal properties of the layer V neurons rat SI cortex, we did not distinguish between neurons recorded in either sublayer. It could be argued that if we were recording primarily from layer Va neurons it would be difficult to get a reasonable estimate of microwire positions used in our analyses.

We feel that it is unlikely that these potential sublaminar differences complicate the analyses or interpretations of our results. First, for the vast majority of our neurons, there was a clear and distinct preference for one whisker, both in terms of strongest response and shortest latency, as reported previously for layer V neurons (Simons, 1978; Ito, 1985; Chapin, 1986). In these previous studies, the PW of the layer V neurons was identical to the PW of neurons recorded directly above it (i.e. the layer IV 'barrel' neurons) (Simons, 1978; Chapin, 1986). Second, it is difficult to isolate clear single units from the smaller layer Va neurons even using sharp electrodes (1–3 μm in tip diameter) (Chapin, 1986), let alone the blunt-tipped, 50 μm microwires used in the present study. Third, our analysis of the center–surround organization of our sample revealed that the differences between center versus surround responses (both magnitude and latency) were extremely large using our criteria (see Fig. 3). Such large differences in average response magnitude would not be apparent if we were recording primarily from layer Va (Armstrong-James *et al.*, 1992). Therefore, it is likely that our recordings are primarily from the large, layer Vb neurons.

As alluded to above, anesthesia may influence the measure-

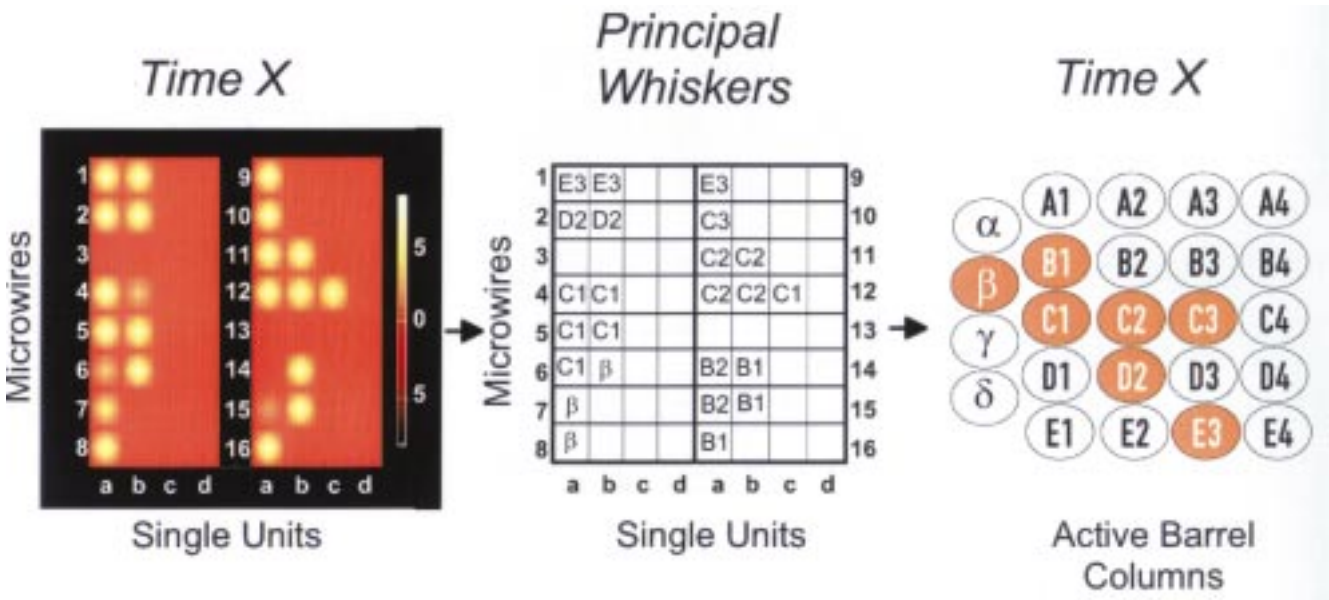

Figure 10. Translation of microwire array activity into barrel field coordinates. The principal whisker of each neuron on each microwire was used to map the location of the microwire in layer V of the barrel cortex. This allowed us to map the spread of whisker-evoked activity across the sampled area of cortex. (Left panel) Raw activity on each of the microwires following a single-whisker deflection. Each array consisted of two rows of eight microwires (1–8 and 9–16) and up to four neurons could be discriminated per microwire (a–d). The scale bar represents standard deviations above baseline activity. For each of the eight 4 ms post-stimulus time epoch, the location of each neuron was mapped according to its principal whisker (middle panel) and then remapped onto a graphical representation of the barrel field (right panel). Neural activity on each of the microwires was considered significant if it exceeded 4 SDs above baseline activity (100 ms pre-stimulus).

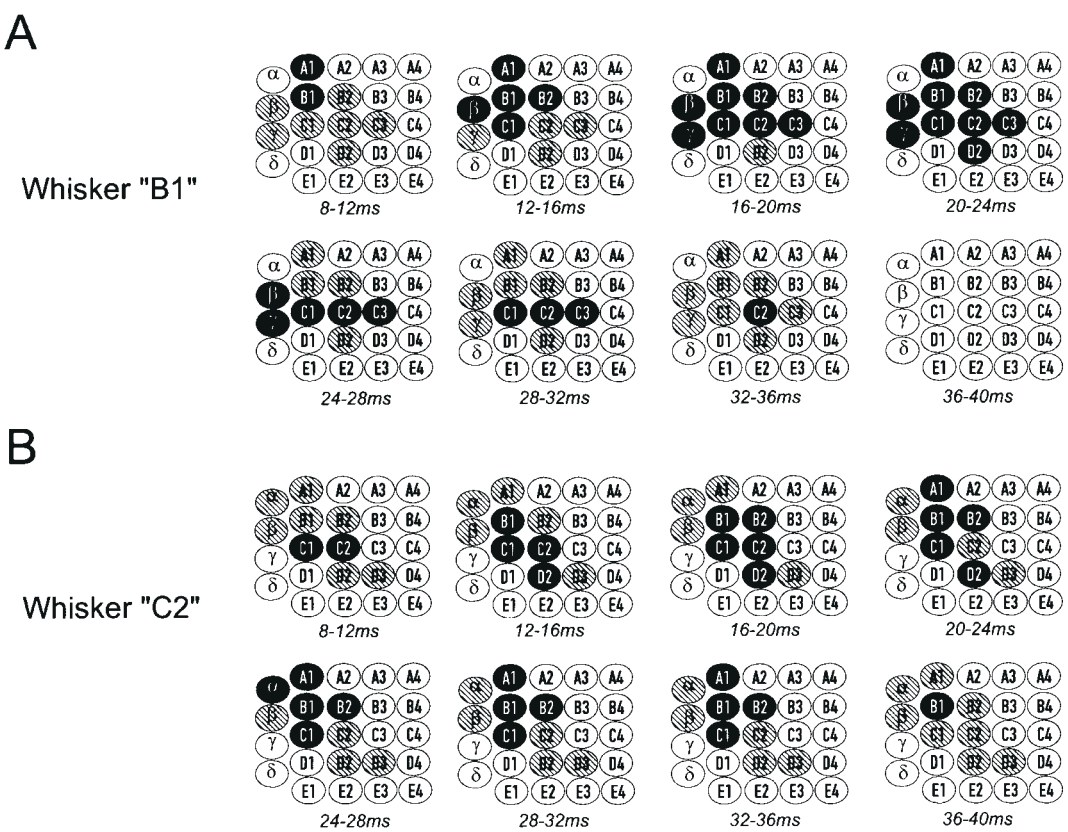

Figure 11. Spread of activity across layer V of SI cortex following single-whisker deflections. By translating the activity of our microwire locations into barrel field coordinates, we were able to map the recruitment of barrel cortical columns over post-stimulus time (see Fig. 10). Each barrel field map depicts the number of active barrel columns (shaded in gray) in a 4ms post-stimulus time epoch. The hatched barrels indicate which barrel cortical columns were sampled by our electrode arrays in these two cases. (*A*) Deflection of whisker B1 elicits large-scale activity across many neurons. The spread of activity moves in both dorsal–ventral and rostral–caudal dimensions. The activity seems to peak in the 20–24 ms time epoch. (*B*) In a different animal, stimulation of whisker C2 also elicits large-scale activity that extends much beyond the C2 barrel cortical column. The peak of activity in this example also occurs in the 20–24 ms post-stimulus time epoch.

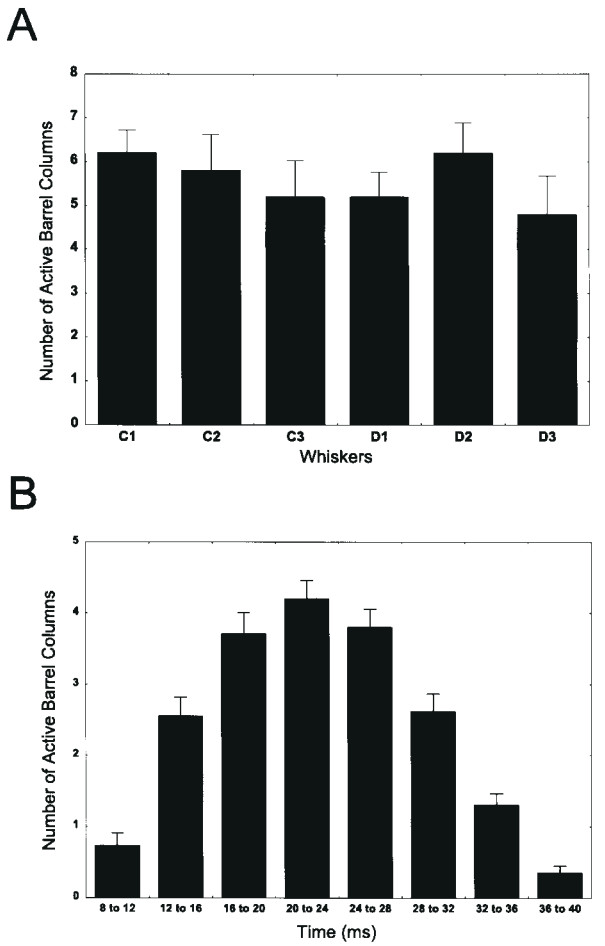

Figure 12. (*A*) Spatial activation of layer V of SI cortex. We quantified the peak number of barrel cortical columns activated in any given post-stimulus time epoch for whiskers in the C and D rows and averaged them across five animals. It can be seen that, using only this spatial analysis, there were no significant differences between the number of barrel cortical columns activated by any of the six whiskers. (*B*) Temporal evolution of SI cortical activation. We quantified the average number of barrel cortical columns activated in each of eight 4 ms post-stimulus time epochs by pooling the responses to the six whiskers of the C and D rows across five animals. The peak of activation occurred in the 20–24 ms post-stimulus time epoch. Error bars are 1 SEM.

ment of responses to whisker deflections. Our recordings were obtained from rats under pentobarbital anesthesia. It has been shown that under conditions similar or identical to those of the present study, pentobarbital anesthesia can decrease the size of RFs relative to the awake condition, while the basic RF structure remains (i.e. the location of centers) remarkably similar (Chapin and Lin, 1984; Nicolelis and Chapin, 1994). Thus, our analyses of the response properties of layer V neurons probably underestimate the full range of their dynamic characteristics. In light of this, the anesthetic state may be used to limit the repertoire of physiological responses of cortical neurons so that only the most robust properties can be readily identified (Chapin and Lin, 1984).

Functional Asymmetries in the Barrel Cortex

The first important finding in this study was the identification of a robust spatial gradient of excitation in layer V of SI cortex where SWs ventral and caudal to the PW had response magnitudes greater than SWs dorsal and rostral to the PW. This layer V activity gradient is consistent with the functional asymmetries seen in the supragranular and granular layers of SI cortex. Studies using 2DG to map use-dependent activity patterns in mice have established that uptake of 2DG is greatest in layer IV barrels corresponding to the ventral and caudal whiskers, and least in barrels of the rostral whiskers (Durham and Woolsey, 1985; McCasland and Woolsey, 1988). Similarly, Simons and colleagues have revealed a spatial gradient of inhibition by applying sequential dual-whisker stimuli (Simons, 1985; Simons and Carvell, 1989; Brumberg *et al.*, 1996). In these studies, a PW deflection, preceded by a deflection of an adjacent caudal/ventral SW, suppresses the PW response more than a rostral/caudal SW. Interestingly, in these studies, the infragranular layers show the least amount of 2DG uptake, and cross-whisker inhibition is not as frequently observed, leading to the conclusion that spatial gradients are minimal in these layers of cortex (McCasland *et al.*, 1991). To our knowledge, no one has reported a spatial gradient of excitation simply by using the excitatory responses of surround whiskers in any cortical layer or subcortical structure like that described here for layer V neurons.

One interesting hypothesis is that these activity gradients are established by experience-dependent mechanisms, whereby those whiskers that get used most frequently will result in a magnification of their representations in SI cortex by increasing the responsiveness of neurons (Armstrong-James *et al.*, 1994; Nicolelis *et al.*, 1996) and the amount of cortical activation devoted to encode responses derived from stimuli applied to them. Experimental approaches which eliminate or perturb active whisker movements, such as neonatal facial nerve cuts (Nicolelis *et al.*, 1996), are currently being carried out in our laboratory to test the dependence of such spatial activity gradients on experience or whether they are established prenatally.

Spatial and Temporal Receptive Field Properties of Layer V Neurons in SI Cortex

Similar to previous studies, our quantitative investigation of receptive field size revealed that most layer V neurons have large (8.5 whiskers), asymmetrical RFs – much larger than neurons in the granular or supragranular layers whose RFs also tend to extend across rows of whiskers (Simons, 1978; Chapin, 1986; Armstrong-James and Fox, 1987). Although most of these studies have focused only on the spatial aspects of RFs (Simons, 1978; Ito, 1981; Chapin, 1986), it is now clear that there is an important temporal component to somatosensory RFs across most of the rodent somatosensory pathway. We observed that the minimal latencies for whiskers that make up such RFs were significantly shorter for PWs than for SWs. In our data, there was no robust pattern to the latency organization of SWs like the pattern found for response magnitude, but some rostral SWs tended to respond at longer latencies than caudal whiskers. Thus, following PW stimulation, the SW that would respond next with the greatest response magnitude varied from neuron to neuron. Similar results have been reported for the granular layer of the rat SI cortex, where it has been demonstrated that the PW response of a barrel neuron has a much shorter latency than its responses to adjacent SWs (Armstrong-James and Fox, 1987; Armstrong-James *et al.*, 1992).

The conjunction of space and time in our RF analyses allowed us to define 'spatiotemporal' RFs for most layer V cortical neurons (Dinse *et al.*, 1991; DeAngelis *et al.*, 1993; Nicolelis and Chapin, 1994). We found that for the majority of neurons in layer V, the center of a neuron's RF shifts as a function of post-stimulus time. Our analysis of the spatiotemporal structure of layer V RFs revealed that they had a variety of directional biases and

complexities. This finding is consistent with previous reports that layer V neurons do not have spatially symmetric RFs; indeed, Chapin (Chapin, 1986) reported a large variety of RF types in layer V, including multi-peaked RFs. Fundamentally, any latency difference between center versus surround RFs defines a 'spatiotemporal' RF provided that the RF center does not remain the same over post-stimulus time. Thus, the presence of strong inhibition, driven by stimulation of the PW, and surround inhibitory gradients, also contribute to the shaping of spatiotemporal RFs. Therefore, we believe that all layers of rat SI cortex should exhibit such dynamic RFs. For ventral posterior medial (VPM) neurons, Nicolelis and Chapin (Nicolelis and Chapin, 1994) also reported spatiotemporal RFs, but these neurons had RFs that shifted primarily in only one direction, caudal to rostral. The difference between layer V and VPM probably represents both nature and complexity of the inputs into these structures, and also suggests the possibility of a thalamocortical transformation of information via intracortical circuitry. The existence of such time-dependent changes in RF structure suggests that single neuronal RFs in both the somatosensory thalamus and SI cortex are dynamic representations of the whisker pad containing both spatial and temporal domains.

Dynamic RF properties have been revealed in a variety of sensory systems. In the visual system, dynamic RFs have been reported for the center–surround/on–off properties (Stevens and Gerstein, 1976; Dinse *et al.*, 1991; DeAngelis *et al.*, 1993; Golomb *et al.*, 1994), end-stopping (Dinse *et al.*, 1991) and orientation tuning of visual neurons (Dinse *et al.*, 1991; Ringach *et al.*, 1997). In the auditory cortex, several studies have demonstrated that auditory neurons have 'spectro-temporal' receptive fields, i.e. the frequency tuning shows selectivity for two or more distinct and separate frequencies and the responses to the multiple peaks often occurred at different latencies (Abeles and Goldstein, 1972; deCharms *et al.*, 1998; Sutter and Schreiner, 1991; Tramo *et al.*, 1996). Our data fit neatly into the picture described by these researchers and provide support for our previous claim that the somatosensory system is no exception: spatiotemporal RFs should be present at multiple levels of this pathway (Nicolelis and Chapin, 1994; Faggin *et al.*, 1997).

Dynamic Receptive Fields: Optimized for Natural Whisking Inputs?

In general, the structure of dynamic RFs in the auditory and visual system corresponds to the spatial/spectral and temporal ranges of behaviorally relevant signals. Neurons with dynamic RFs could therefore act as combination-sensitive integrators of complex, time-varying sensory inputs. This hypothesis has been supported by recent studies in which natural vocalizations (Rauschecker *et al.*, 1995; Tramo *et al.*, 1996) and synthetic 'optimized' signals (deCharms *et al.*, 1998), corresponding to the spectro-temporal structure of each neuron's RF, resulted in supralinear responses. We hypothesize that the spatiotemporal RFs of layer V SI cortical neurons in the rat probably relate to the complex patterns of whisker deflections that occur during active whisking of surfaces during exploratory behaviors. In the VPM, spatiotemporal RFs can be radically altered by preventing the rat from actively whisking during postnatal development (Nicolelis *et al.*, 1996); in fact, the dynamic nature of these RFs is often eliminated altogether. Thus, experience in the form of active whisking appears to play an important role in defining the structure of spatiotemporal RFs.

What are the functions of spatiotemporal RFs? We have hypothesized that they could act as combination-sensitive integrators of multiwhisker inputs. We have already reported that simultaneous deflections of whiskers results in supralinear responses in both thalamic and layer V cortical neurons (Ghazanfar and Nicolelis, 1997); therefore, a further prediction is that time-varying stimuli optimized for a particular spatiotemporal RF, where the pattern of whisker inputs is mapped to the time-dependent RF structure, will also result in a supralinear cortical response. Further experiments in the awake animal using more complex stimuli will also be necessary to test these hypotheses.

Asynchronous Convergence of Multiple Inputs: Potential Substrates for Somatosensory RFs

The dynamic nature of the RFs suggests the convergence of asynchronous inputs onto layer V SI neurons. Possible feedforward pathways include parallel inputs from the lemniscal and paralemniscal somatosensory pathways which have different temporal lags. The faster, lemniscal pathway could involve direct, monosynaptic connections from VPM to layer V SI cortical neurons (Agmon and Connors, 1992), while the slower, paralemniscal pathway could involve both the VPM and the posterior medial nucleus of the thalamus which has extensive terminations in layer V. Both of these thalamic nuclei have large, multiwhisker RFs (Diamond *et al.*, 1992; Nicolelis and Chapin, 1994). Intracortically, local or inter-areal connections could also participate in the genesis of the RF properties seen in our data. Axonal arbors of layer V neurons can project up to 2 mm and in many directions (Hoeflinger *et al.*, 1995; Gottlieb and Keller, 1997). Unlike layer IV neurons (Simons and Woolsey, 1984), the dendritic arbors of layer V neurons extend across more than one barrel column, and thus may receive inputs from more than one 'barreloid' from VPM (Ito, 1992; Gottlieb and Keller, 1997). Finally, feedback connections from other somatosensory areas may also contribute to the spatiotemporal RF structure of layer V neurons (Koralek *et al.*, 1990; Fabri and Burton, 1991). The 'asynchronicity' hypothesis for the genesis of spatiotemporal RFs could be tested by inactivating either the feedforward inputs to SI cortex from the periphery or by inactivation of different cortical areas projecting to SI cortex. Experiments similar to these have supported this hypothesis for the genesis of VPM spatiotemporal RFs (Nicolelis *et al.*, 1993b; Ghazanfar *et al.*, 1997).

Spatial and Temporal Characteristics of Large-scale Cortical Activation

In many neural network models, activation of large distributed networks of neural elements with extensive feedback provides the anatomical substrate for the classification of various stimulus features. In fact, the dynamic trajectory of activity across the network becomes the computation itself. As a first step towards studying real biological networks from a similar vantage point, we analyzed the spatial and temporal pattern of cortical activation across a 2 mm^2 region in layer V of SI cortex in response to single-whisker deflections. We found that such a punctate stimulus activates a large portion of SI cortex, and that this sensory evoked neural activity extends well beyond the barrel cortical column of the PW. Consistent with anatomical studies of local projections (Ito, 1992; Hoeflinger *et al.*, 1995; Gottlieb and Keller, 1997), there did not appear to be any bias of activation in any particular direction of spread like that seen in layers II/III where the tangential spread of activity is elongated along representations of whisker rows (Kleinfeld and Delaney, 1996). Although there were no differences in the maximum number of

barrel cortical columns recruited at any given epoch, the inclusion of time as a parameter may reveal differences between the spatiotemporal pattern of cortical activation. Similar analyses, using serial reconstruction of single unit activity, have been performed for layer IV activation (Armstrong-James *et al.*, 1992). However, consistent with the intracortical anatomy of layer IV, they found that there is only a small spread of cortical activity laterally beyond the barrels.

Several studies using optical imaging have demonstrated that, despite the presence of an elegant one whisker–one barrel anatomical organization of rat SI cortex seen in anatomical studies (Killackey, 1973), single-whisker deflections elicit activity that extends beyond just a single barrel column (Kleinfeld and Delaney, 1996; Masino and Frostig, 1996; Peterson *et al.*, 1998). In these experiments, activity may spread tangentially for almost 2 mm^2 (Masino and Frostig, 1996) — the maximum spatial resolution of our approach. The present results extend previous findings by comparing the amount of action-potential activity in layer V elicited by different whiskers. In imaging studies, the relationship between the imaged signal and action-potential activity has not yet been established, and it is not clear what cortical layer(s) is being imaged [see Kleinfeld and Delaney (Kleinfeld and Delaney, 1996) for more discussion on this point]. Moreover, analysis of the temporal component of the imaged activity is not possible on a millisecond timescale. Our use of single-unit, microwire-array physiology obviated these problems and allowed us to clearly demonstrate and quantify the spatiotemporal spread of action-potential activity across layer V of SI cortex.

Conclusions

The experimental evidence reviewed in this paper indicates that sensory processing is likely to be the outcome of highly distributed interactions between populations of broadly tuned neurons dispersed throughout the multiple and reciprocally connected subcortical and cortical areas that define the somatosensory system. Therefore, we propose that, at least to a first approximation, the SI cortex of the rat does not operate as a static decoder of passive whisker information; instead, the properties of its neurons are spatiotemporally complex and seem to reflect the dynamic nature of active sensory processing related to the exploratory behaviors used by rats. We further hypothesize that during adulthood, the spatiotemporal organization of the somatosensory system reflects its active attempt, during exploratory behaviors, to compare the meaning encoded into a time-varying stimulus with the accumulated representations of the sensory experiences acquired during a lifetime.

Notes

We thank Don Katz for a critical reading of this manuscript, and Mark Laubach and Marshal Shuler for programming and helpful advice on analyses. We also would like to thank the three anonymous reviewers for their helpful comments on this manuscript.This work was supported by the Whitehall Foundation and the National Institute for Dental Research (DE-11121–01).

Address correspondence to Miguel Nicolelis, Department of Neurobiology, Box 3209, Duke University Medical Center, Durham, NC 27710, USA. Email: nicolelis@neuro.duke.edu.

References

Abeles M, Goldstein M (1977) Multispike train analysis. IEEE Proc 65:762–773.

Abeles M, Goldstein MH (1972) Responses of single units in the primary auditory cortex of the cat to tones and to tone pairs. Brain Res 42:337–352.

Agmon A, Connors BW (1992) Correlation between intrinsic firing patterns and thalamocortical synaptic responses of neurons in mouse barrel cortex. J Neurosci 12:319–329.

Amitai Y, Connors BW (1995) Intrinsic physiology and morphology of single neurons in neocortex. In: Cerebral cortex (Jones EG, Diamond IT, eds), Vol. 11, pp. 299–331. New York: Plenum.

Armstrong-James M, Fox K (1987) Spatiotemporal convergence and divergence in the rat SI 'barrel' cortex. J Comp Neurol 263:265–281.

Armstrong-James M, Fox K, Das-Gupta A (1992) Flow of excitation within rat barrel cortex on striking a single vibrissa. J Neurophysiol 68: 1345–1358.

Armstrong-James M, Diamond ME, Ebner FF (1994) An innocuous bias in whisker use in adult rats modifies receptive fields of barrel cortex neurons. J Neurosci 14:6978–6991.

Brumberg JC, Pinto DJ, Simons DJ (1996) Spatial gradients and inhibitory summation in the rat whisker barrel system. J Neurophysiol 76:130–140.

Carvell GE, Simons DJ (1990) Biometric analyses of vibrissal tactile discrimination in the rat. J Neurosci 10:2638–2648.

Carvell GE, Simons DJ (1996) Abnormal tactile experience early in life disrupts active touch. J Neurosci 16:2750–2757.

Chapin JK (1986) Laminar differences in sizes, shapes, and response profiles of cutaneous receptive fields in the rat SI cortex. Exp Brain Res 62:549–559.

Chapin JK, Lin CS (1984) Mapping the body representation in the SI cortex of anesthetized and awake rats. J Comp Neurol 229:199–213.

Chmielowska J, Carvell GE, Simons DJ (1989) Spatial organization of thalamocortical and corticothalamic projection systems in the rat SmI barrel cortex. J Comp Neurol 285:325–338.

Connors BW, Amitai Y (1995) Functions of local circuits in neocortex: synchrony and laminae. In: The cortical neuron (Gutnick MJ, Mody I, eds), pp. 123–140. New York: Oxford University Press.

Damasio H, Grabowski TJ, Tranel D, Hichwa RD, Damasio AR (1996) A neural basis for lexical retreival. Nature 380:499–505.

DeAngelis GC, Ohzawa I, Freeman RD (1993) Spatiotemporal organization of simple-cell receptive fields in the cat's striate cortex. I. General characteristics and postnatal development. J Neurophysiol 69:1118–1135.

deCharms RC, Blake DT, Merzenich MM (1998) Optimizing sound features for cortical neurons. Science 280:1439–1443.

Diamond ME, Armstrong-James M, Budway MJ, Ebner FF (1992) Somatic sensory responses in the rostral sector of the posterior group (POm) and in the ventral posterior medial nucleus (VPM) of the rat thalamus. J Comp Neurol 318:462–476.

Dinse HR, Kruger K, Mallot HA, Best J (1991) Temporal structure of cortical information processing: cortical architecture, oscillations, and non-separability of spatio-temporal receptive field organization. In: Neuronal cooperativity (Kruger J, ed.), pp. 68–104. Berlin: Springer-Verlag.

Durham D, Woolsey TA (1985) Functional organization in cortical barrels of normal and vibrissae-damaged mice: a (3-H) 2-deoxyglucose study. J Comp Neurol 235:97–110.

Erickson RP (1986) A neural metric. Neurosci Biobehav Rev 10:377–386.

Fabri M, Burton H (1991) Ipsilateral cortical connections of primary somatic sensory cortex in rats. J Comp Neurol 311:405–424.

Faggin BM, Nguyen KT, Nicolelis MA (1997) Immediate and simultaneous sensory reorganization at cortical and subcortical levels of the somatosensory system. Proc Natl Acad Sci USA 94:9428–9433.

Ghazanfar AA, Nicolelis MAL (1997) Nonlinear processing of tactile information in the thalamocortical loop. J Neurophysiol 78:506–510.

Ghazanfar AA, Krupa DJ, Nicolelis MAL (1997) Tactile processing by thalamic neural ensembles: the role of cortical feedback. Soc Neurosci Abstr 1797.

Gil Z, Amitai Y (1996) Properties of convergent thalamocortical and intracortical synaptic potentials in single neurons of neocortex. J Neurosci 16:6567–6578.

Golomb D, Kleinfeld D, Reid RC, Shapley RM, Shraiman BI (1994) On temporal codes and the spatiotemporal response of neurons in the lateral geniculate nucleus. J Neurophysiol 72:2990–3003.

Gottlieb JP, Keller A (1997) Intrinsic circuitry and physiological properties of pyramidal neurons in rat barrel cortex. Exp Brain Res.

Hoeflinger BF, Bennett-Clarke CA, Chiaia NL, Killackey HP, Rhoades RW (1995) Patterning of local intracortical projections within the vibrissae representation of rat primary somatosensory cortex. J Comp Neurol 354:551–563.

Hutson KA, Masterton RB (1986) The sensory contribution of a single vibrissa's cortical barrel. J Neurophysiol 56:1196–1223.
Ito M (1981) Some quantitative aspects of vibrissa-driven neuronal responses in rat neocortex. J Neurophysiol 46:705–715.
Ito M (1985) Processing of vibrissa sensory information within rat neocortex. J Neurophysiol 54:479–490.
Ito M (1992) Simultaneous visualization of cortical barrels and horseradish peroxidase-injected layer 5b vibrissa neurones in the rat. J Physiol 454:247–265.
Killackey HP (1973) Anatomical evidence for cortical subdivisions based on vertically discrete thalamic projections from the ventral posterior nucleus to cortical barrels in the rat. Brain Res 51:326–331.
Killackey HP, Koralek K-A, Chiaia NL, Rhoades RW (1989) Laminar and areal differences in the origin of the subcortical projection neurons of the rat somatosensory cortex. J Comp Neurol 282:428–445.
Kleinfeld D, Delaney KR (1996) Distributed representation of vibrissa movement in the upper layers of somatosensory cortex revealed with voltage-sensitive dyes. J Comp Neurol 376:89–108.
Koralek K-A, Olavarria J, Killackey HP (1990) Areal and laminar organization of corticocortical projections in the rat somatosensory cortex. J Comp Neurol 299:133–150.
MacPherson JM, Aldridge JW (1979) A quantitative method of computer analysis of spike train data collected from behaving animals. Brain Res 175:183–187.
Markram H (1997) A network of tufted layer 5 pyramidal neurons. Cereb Cortex 7:523–533.
Masino SA, Frostig RD (1996) Quantitative long-term imaging of the functional representation of a whisker in rat barrel cortex. Proc Natl Acad Sci USA 93:4942–4947.
McCasland JS, Woolsey TA (1988) High-resolution 2-deoxyglucose mapping of functional cortical columns in mouse barrel cortex. J Comp Neurol 278:555–569.
McCasland JS, Carvell GE, Simons DJ, Woolsey TA (1991) Functional asymmetries in the rodent barrel cortex. Somatosens Motor Res 8:111–116.
Merzenich MM, Jenkins WM, Johnston P, Schreiner C, Miller SL, Tallal P (1996) Temporal processing deficits of language-learning impaired children ameliorated by training. Science 271:77–81.
Nicolelis MAL, Chapin JK (1994) Spatiotemporal structure of somatosensory responses of many-neuron ensembles in the rat ventral posterior medial nucleus of the thalamus. J Neurosci 14:3511–3532.
Nicolelis MAL, Lin RC, Woodward DJ, Chapin JK (1993a) Dynamic and distributed properties of many-neuron ensembles in the ventral posterior medial thalamus of awake rats. Proc Natl Acad Sci USA 90:2212–2216.
Nicolelis MAL, Lin RCS, Woodward DJ, Chapin JK (1993b) Induction of immediate spatiotemporal changes in thalamic networks by peripheral block of ascending cutaneous information. Nature 361:533–536.
Nicolelis MAL, Oliveira LMO, Lin RCS, Chapin JK (1996) Active tactile exploration influences the functional maturation of the somatosensory system. J Neurophysiol 75:2192–2196.
Nicolelis MAL, Ghazanfar AA, Faggin BM, Votaw S, Oliveira LMO (1997) Reconstructing the engram: simultaneous, multisite, many single neuron recordings. Neuron 18:529–537.
Peterson BE, Goldreich D, Merzenich MM (1998) Optical imaging and electrophysiology of rat barrel cortex. I. responses to small single-vibrissa deflections. Cereb Cortex 8:173–183.
Rauschecker JP, Tian B, Hauser M (1995) Processing of complex sounds in the macaque nonprimary auditory cortex. Science 268:111–114.
Richmond BJ, Optican LM, Podell M, Spitzer H (1987) Temporal encoding of two-dimensional patterns by single units in primate inferior temporal cortex. I. Response characteristics. J Neurophysiol 57:132–146.
Riddle DR, Purves D (1995) Individual variation and lateral asymmetry of the rat primary somatosensory cortex. J Neurosci 15:4184–4195.
Ringach DL, Hawken MJ, Shapley RM (1997) Dynamics of orientation tuning in macaque primary visual cortex. Nature 387:281–284.
Schwindt P, O'Brien JA, Crill W (1997) Quantitative analysis of firing properties of pyramidal neurons from layer 5 of rat sensorimotor cortex. J Neurophysiol 77:2484–2498.
Simons DJ (1978) Response properties of vibrissa units in rat SI somatosensory neocortex. J Neurophysiol 41:798–820.
Simons DJ (1985) Temporal and spatial integration in the rat SI vibrissa cortex. J Neurophysiol 54:615–635.
Simons DJ, Carvell GE (1989) Thalamocortical response transformation in the rat vibrissa/barrel system. J Neurophysiol 61:311–330.
Simons DJ, Carvell GE, Hershey AE, Bryant DP (1992) Response of barrel cortex neurons in awake rats and effects of urethane anesthesia. Exp Brain Res 91:259–272.
Stevens JK, Gerstein GL (1976) Spatiotemporal organization of cat lateral geniculate receptive fields. J Neurophysiol 39:213–238.
Sutter ML, Schreiner CE (1991) Physiology and topography of neurons with multipeaked tuning curves in cat primary auditory cortex. J Neurophysiol 65:1207–1226.
Tramo MJ, Bellew BF, Hauser MD (1996) Discharge patterns of auditory cortical neurons evoked by species-specific vocalizations and synthetic complex signals in alert *Macaca mulatta*. Soc Neurosci Abstr 1623.
Wise SP, Jones EG (1977) Cells of origin and terminal distribution of descending projections of the rat somatic sensory cortex. J Comp Neurol 176:129–158.
Woolsey TA, Van der Loos H (1970) The structural organization of layer IV in the somatosensory region (SI) of mouse cerebral cortex: the description of a cortical field composed of discrete cytoarchitectonic units. Brain Res 17:205–242.
Zheng D, Purves D (1995) Effects of increased neural activity on brain growth. Proc Natl Acad Sci USA 92:1802–1806.